

# The C1 Domain of Protein Kinase C as a Lipid Bilayer Surface Sensing Module<sup>†</sup>

Cojen Ho, Simon J. Slater, Brigid Stagliano, and Christopher D. Stubbs\*

Department of Pathology, Anatomy, and Cell Biology, Thomas Jefferson University, Philadelphia, Pennsylvania 19107

Received December 14, 2000; Revised Manuscript Received June 5, 2001

**ABSTRACT:** The activity of membrane-associated protein kinase C (PKC) is tightly controlled by the physical properties of the membrane lipid bilayer, in particular, curvature stress, which is induced by bilayer-destabilizing lipid components. An important example of this is the weakened lipid headgroup interactions induced by phosphatidylethanolamine (PE) and cholesterol. In this work our previous observation with a mixed isoform PKC showing a biphasic dependence of activity as a function of membrane curvature stress [Slater et al. (1994) *J. Biol. Chem.* 269, 4866–4871] was here extended to individual isoforms. The Ca<sup>2+</sup>-dependent PKC $\alpha$ , PKC $\beta$ , and PKC $\gamma$ , along with Ca<sup>2+</sup>-independent PKC $\delta$ , but not PKC $\epsilon$  or PKC $\zeta$ , displayed a biphasic activity as a function of membrane PE content. The fluorescence anisotropy of *N*-(5-dimethylaminonaphthalene-1-sulfonyl)dioleoylphosphatidylserine (dansyl-PS), which probes the lipid environment of PKC, also followed a biphasic profile as a function of PE content for full-length PKC $\alpha$ , PKC $\beta$ II, and PKC $\gamma$  as did the isolated C1 domain of PKC $\alpha$ . In addition, the rotational correlation time of both PKC $\alpha$  and PKC $\delta$  C1-domain-associated sapintoxin D, a fluorescent phorbol ester, was also a biphasic function of membrane lipid PE content. These results indicate that the C1 domain acts as a sensor of the bilayer surface properties and that its conformational response to these effects may directly underlie the resultant effects on enzyme activity.

Protein kinase C (PKC)<sup>1</sup> is a key enzyme in the regulation of cell signaling (reviewed refs 1–4). There are 12 major isoforms known: Ca<sup>2+</sup>-dependent cPKC (e.g., PKC $\alpha$ , PKC $\beta$ I/II, and PKC $\gamma$ ), Ca<sup>2+</sup>-independent nPKC (e.g., PKC $\delta$  and PKC $\epsilon$ ), and diacylglycerol/phorbol ester-independent aPKC (e.g., PKC $\zeta$ ) isoforms. The activation of membrane-associated PKC proceeds in two discrete stages. These are *translocation* to the membrane and *activation* which proceeds via an *activating conformational change* (5), the final level of activation attained being a function of the membrane lipid composition which involves protein–lipid interactions with the regulatory domain (reviewed in refs 4 and 6) and the presence of multiple activators (7–9). Although considerable detail concerning the role of membrane lipid composition in PKC activation is known, which part of the PKC regulatory domain constitutes the lipid sensing module and how it regulates activity remain to be determined.

A number of studies have shown that the presence of PE in a lipid bilayer increases the activity of PKC (see, for example, refs 5 and 10–14), cholesterol having a similar

effect (5, 14, 15). In cells having PE deficiency an abnormal function of PKC is found (16), and activity is elevated in liver plasma membranes enriched with PE (17) and cholesterol (18). The mechanism involves effects on lipid curvature stress, which is increased by the presence of PE and cholesterol (reviewed in ref 6). Other examples of effects of nonbilayer lipids on membrane proteins and related functions would include a modulation of phospholipase A2 activity (19–23), facilitation of fusion and transport (24, 25), modulation of the insertion of the antimicrobial peptide magainin 2 (26), stability of gramicidin tryptophan–lipid contacts (27), modulation of the sterol carrier protein-2 N-terminus membrane-binding domain (28), induction of conformational changes in cytochrome *c* (29), formation of influenza virus-mediated fusion pores (30), and a correlation between the free energy of a channel-forming voltage-gated peptide and the spontaneous curvature (31) (also reviewed in refs 6, 23, 32, and 33). Despite these varied effects the molecular mechanism(s) have remained unknown.

Due to the overall cone shape of PE with the headgroup being the narrow end, there is a tendency to form tightly curved (nonbilayer) structures that would be incompatible with a (planar) bilayer so that the maintenance of the latter introduces a strain or stored energy in the headgroup region. The energy stored in the bilayer as a result of this effect is referred to as “curvature stress” or “spontaneous curvature”. The spontaneous curvature is the curvature that one monolayer will assume if allowed to bend freely, independent of the constraints imposed by the opposite monolayer of the bilayer, and is quantified as the spontaneous radius of curvature. The curvature stress that facilitates insertion of proteins such as PKC into the headgroup region provides free energy and drives conformational changes in proteins

<sup>†</sup>This work was supported by U.S. Public Health Service Grants AA08022, AA07215, AA07186, and AA07465.

\* Corresponding author: Department of Pathology, Anatomy, and Cell Biology, Room 271 JAH, Thomas Jefferson University, 1020 Locust St., Philadelphia, PA 19107. Telephone: (215) 503-5019. Fax: (215) 923-2218. E-mail: Chris.Stubbs@mail.tju.edu.

<sup>1</sup> Abbreviations: BPS, brain phosphatidylserine; DAG, dioleoyl-*sn*-glycerol; dansyl-PS, *N*-(5-dimethylaminonaphthalene-1-sulfonyl)dioleoylphosphatidylserine; EDTA, ethylenediaminetetraacetic acid; EGTA, ethylene glycol bis( $\beta$ -aminoethyl ether)-*N,N,N',N'*-tetraacetic acid; GST, glutathione *S*-transferase; LUV, large unilamellar vesicles; PKC, protein kinase C; POPC, 1-palmitoyl-2-oleoylphosphatidylcholine; POPE, 1-palmitoyl-2-oleoylphosphatidylethanolamine; RET, resonance energy transfer; SAPD, sapintoxin D [12-(*N*-methylantraniloyl)phorbol-13-acetate]; TPA, 4 $\beta$ -12-*O*-tetradecanoylphorbol-13-acetate.

(6, 34, 35). Which region senses the curvature stress remains unknown, not only for PKC but for any membrane protein.

In a previous study we showed, with a rat brain cPKC isoform mixture, that increasing the level of PE in membranes increases the level of PKC activity to a maximum after which further increases in PE lead to decline in activity (14). It was concluded that while insertion into the membrane is facilitated by increased PE, there is a specific *level* of PE that accommodates an *optimal* conformation of PKC that displays *maximal* activity. Thus, higher or lower levels of PE would accommodate conformations of the enzyme that are suboptimal in terms of activity. The isoform specificity of this effect and the region sensing the curvature stress have remained to be determined.

The present study was undertaken with two aims. The first was to determine if the effects of bilayer destabilizing components exemplified by PE on the activity of the major PKC isoforms followed a similar biphasic dependence. The second was to determine which region of the PKC represents the bilayer sensing module. It was found that while all PKC isoforms responded to bilayer destabilizing effects of PE, PKC $\alpha$ , PKC $\beta$ II, PKC $\gamma$ , and PKC $\delta$ , but not PKC $\epsilon$  or PKC $\zeta$ , displayed activities that were a *biphasic* function of PE content. Evidence also is presented showing that the sensitivity of PKC activity to membrane surface curvature stress is controlled by the C1-activator binding module, a domain common to a number of other signaling proteins.

## MATERIALS AND METHODS

**Materials.** All of the phospholipids, 1,2-dioleoyl-*sn*-glycerol (DAG), and dansyl-PS were from Avanti Polar Lipids (Alabaster, AL). The phospholipid concentrations were determined by phosphorus assay (36). 12-(*N*-Methyl-anthraniloyl)phorbol-13-acetate (SAPD) was from Calbiochem (La Jolla, CA), TPA (4 $\beta$ -12-*O*-tetradecanoylphorbol-13-acetate), and cholesterol were from Sigma (St. Louis, MO), and ATP was from Boehringer Mannheim (Indianapolis, IN). [ $\gamma$ - $^{32}$ P]ATP was from DuPont NEN (Boston, MA). Peptide substrates, myelin basic protein (QKRPSQRSKYL, MBP $_{4-14}$ ), and PKC $\epsilon$  pseudosubstrate peptide substrate (with the single alanine residue replaced by serine) were custom synthesized by the Protein Chemistry Facility of the Kimmel Cancer Center at Jefferson. Solvents, analytical grade, were from Fisher Scientific (Pittsburgh, PA) or from Sigma (St. Louis, MO).

**Phospholipid Vesicles.** Large unilamellar vesicles (LUV) were prepared as previously described (37). Briefly, aliquots of the required amounts of lipid in chloroform were placed in a test tube and the solvents removed under a stream of nitrogen. Then 50 mM Tris-HCl (pH 7.4) was added, and the contents were vortexed before being passed through 0.1  $\mu$ m polycarbonate filters using a Avestin Liposofast extruder (Avestin, Ottawa, Canada). LUV consisted of phosphatidylcholine (POPC) and brain phosphatidylserine (BPS) at a 4:1 molar ratio, with and without DAG (4 mol %), cholesterol (0–25 mol %), 1-palmitoyl-2-oleoylphosphatidethanolamine (POPE) (0–80 mol %), and dansyl-PS (2 mol %), the latter included as required to yield a final lipid concentration of 50–100  $\mu$ M as required. SAPD (1  $\mu$ M) in dimethyl sulfoxide (DMSO) was added to preformed vesicles as required. All of the measurements were performed at 30 °C.

**Purification of PKC Isozymes and Subdomains.** Recombinant PKC $\alpha$ , PKC $\beta$ II, PKC $\gamma$ , and PKC $\epsilon$  (rat brain) were prepared using the baculovirus *Spodoptera frugiperda* (Sf9) insect cell expression system (38) and were purified to homogeneity as described elsewhere (39). The isoforms nPKC $\delta$ , nPKC $\epsilon$ , and aPKC $\zeta$  were also overexpressed in Sf9 cells but as fusion proteins containing a (His) $_6$  attached to the C-terminus. The cloning, isolation, and purification of (His) $_6$ -tagged proteins were performed as previously described (39, 40).

For preparation of glutathione *S*-transferase (GST)–C1–(His) $_6$  fusion proteins, based on evidence that GST stabilizes the isolated C1 domain and to ensure the production of only full-length peptides GST–C1–(His) $_6$ , fusion proteins corresponding to PKC $\alpha$  and PKC $\epsilon$  were constructed and isolated as previously described (39, 40). The PKC $\delta$ -C1 plasmid was kindly provided by Dr. Peter Blumberg (41).

**PKC Activity Assay.** The activity of PKC isoforms was determined as previously described (14) using MBP $_{4-14}$  for cPKC or the PKC $\epsilon$  pseudosubstrate peptide (peptide  $\epsilon$ ) for nPKC and PKC $\zeta$ . The assay system consisted of 50 mM Tris-HCl (pH 7.4) containing 0.1 mM Ca $^{2+}$ , 50  $\mu$ M MBP $_{4-14}$ /peptide  $\epsilon$ , and lipid vesicles (150  $\mu$ M) in a total volume of 75  $\mu$ L. After thermal equilibration to 30 °C, assays were initiated by the simultaneous addition of PKC (1 nM) along with a solution containing 5 mM Mg $^{2+}$ , 15  $\mu$ M ATP, and 0.3  $\mu$ Ci of [ $\gamma$ - $^{32}$ P]ATP (3000 Ci/mmol). After 30 min the assay was terminated with 100  $\mu$ L of 175 mM phosphoric acid. Then 100  $\mu$ L was transferred to Whatman P81 filter papers, which were washed three times in 75 mM phosphoric acid, and the radioactivity associated with the phosphorylated peptide was then determined by liquid scintillation counting.

**Determination of PKC Membrane Association.** The PE concentration dependence of the association of PKC $\alpha$ , PKC $\delta$ , and PKC $\alpha$ -C1 with membrane lipid vesicles was determined by centrifugal separation of free from bound protein using sucrose-loaded vesicles (SLV) as previously described (42). Briefly, SLV were prepared by evaporating the required volumes of chloroform solutions of BPS, POPC, and DAG (20:76:4 molar ratio) and varied POPE amount under a stream of nitrogen. Following this, 2 mL of 50 mM Tris-HCl buffer (pH 7.40) containing 170 mM sucrose was placed on top of the dried lipid film to give a total lipid concentration of 3 mM. After hydration was allowed for 10 min at 30 °C, the mixture was vortexed for 1 min to form multilamellar vesicles. Then the sample was subjected to three freeze–thaw cycles using liquid nitrogen. SLV were produced by extrusion through 100 nm filters using a Liposofast extruder. To remove excess sucrose external to the SLV, the vesicles were diluted 4-fold with 50 mM Tris-HCl (pH 7.40) and centrifuged for 30 min at 100000g. The supernatant was then discarded and the SLV pellet resuspended in 6 mL of 50 mM Tris-HCl buffer (pH 7.40) to give a final lipid concentration of 750  $\mu$ M (assuming 100% lipid recovery). To determine losses of lipid during SLV manufacture, the fluorescent phospholipid, N-Rho-PE was codispersed with the lipids at a level of 0.25 mol % of the total lipid concentration. Corrections required for losses of lipid were calculated on the basis of a comparison of the N-Rho-PE emission fluorescence intensity, measured at 530 nm upon excitation at 470 nm, for the phospholipid dispersion formed prior to extrusion with that of the final product. PKC or the

C1 domain (0.1  $\mu$ M) was preincubated (in the presence of the required free  $\text{Ca}^{2+}$  for PKC $\alpha$  and other the activity assay components, as described above) and the SLV at 30 °C for 30 min. This was followed by centrifugation for 1 h at 100000g. Following this, 40  $\mu$ L of the supernatant was removed and the PKC determined by measurement of its activity in the presence LUV and other assay components, as described above. For the PKC $\alpha$ -C1 the amount of protein was directly quantitated using the Bradford assay (Bio-Rad) with bovine serum albumin as the standard.

**Fluorescence Spectroscopy.** Fluorescence data were collected using an SLM 48000 multifrequency phase-modulation fluorometer in the T-format configuration. Steady-state anisotropy was measured, using a Xenon lamp as the excitation source, at 340 nm for dansyl-PS and 355 nm for SAPD. Time-resolved fluorescence measurements were made by a Liconix HeCd laser (model 4240NB, emission 325 nm), sinusoidally modulated by radio frequencies from 5 to 130 MHz. For dansyl-PS the emission was collected through 430 nm red-pass filters and Glan-Thompson polarizers set at the desired orientation(s) for anisotropy measurements. For SAPD 385 nm red-pass filters were used. The principle and operational details were as published elsewhere (43, 44). The experimental errors used in fluorescence lifetime data analysis were the averaged errors over the range of frequency collected in data acquisition, which were of the order of 0.2° in the phase and 0.002 in the modulation. For time-resolved fluorescence anisotropy the averaged experimental errors were usually 0.3° in the phase and 0.003 in the modulation.

**Fluorescence Data Analysis.** Steady-state anisotropy  $r_s$  was calculated according to

$$r_s = I_{VV} - GI_{VH}/I_{VV} + 2GI_{VH}$$

where  $G$  is the instrumental correction factor ( $G = I_{HV}/I_{HH}$ ),  $I_{VV}$  is the emission intensity with vertically polarized excitation and emission, and  $I_{VH}$  is the emission intensity with vertically polarized excitation and horizontally polarized emission. Time-resolved phase and modulation data were analyzed on the basis of  $\chi^2$  and residuals using the Globals Unlimited software (Laboratory of Fluorescence Dynamics, University of Illinois, Urbana-Champaign, IL) (45, 46). It was found that a triple exponential rotational decay was appropriate for SAPD accounting for free SAPD and for lipid- and PKC-bound SAPD, as previously described (5).

## RESULTS

**The Activities of PKC $\alpha$ , PKC $\beta$ II, PKC $\gamma$ , and PKC $\delta$  Are a Biphasic Function of the Vesicle PE Content.** In previous studies the presence of PE has been shown to increase the activity of PKC in lipid vesicle dependent assay systems (10–14). In our earlier study (14) we showed for a rat brain cPKC mixed isoform preparation that activity is a biphasic function of the PE content (in POPC/BPS vesicles)—the activity declining after reaching a maximal value (14). Therefore, an important initial aim of the present study was first to determine the isoform specificity of this effect. The results in Figure 1 show that PKC $\alpha$ , PKC $\beta$ II, PKC $\gamma$ , and PKC $\delta$ , but not PKC $\epsilon$  and PKC $\zeta$ , display a similar biphasic activity profile as a function of the level of PE in the vesicles is increased. We have also explored varying PE polyunsaturation with 1-palmitoyl-2-arachidonyl-PE and found (results

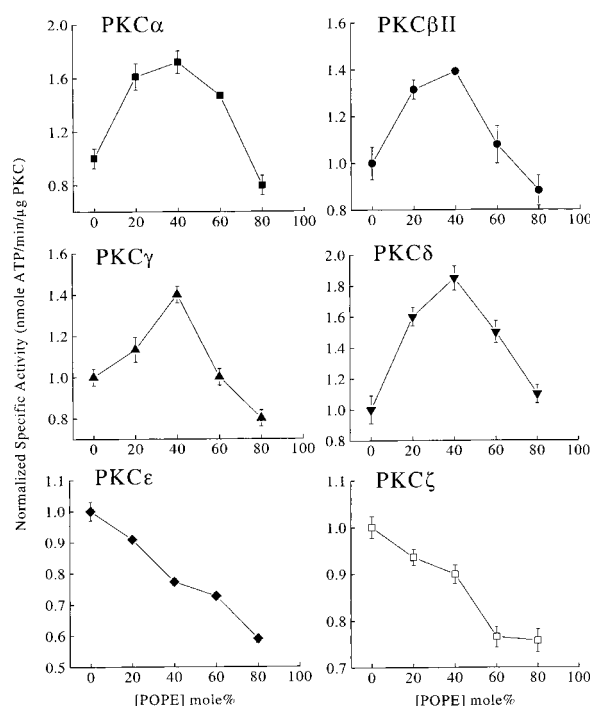


FIGURE 1: PKC specific activities as a function of POPE concentration in vesicles. The specific activities were determined as described under Materials and Methods and are normalized for comparative purposes. Note that enzyme activity is a biphasic function of POPE for PKC $\alpha$  (■), PKC $\beta$ II (●), PKC $\gamma$  (▲), and PKC $\delta$  (▼), with the maximal enzyme activity at the 40 mol % POPE level. Activities of PKC $\epsilon$  (◆) and PKC $\zeta$  (□) did not display a biphasic POPE dependency. The composition for vesicles used is POPC/BPS/DAG (80:20:4, molar) with the POPE incorporated at the expense of POPC. The standard errors were obtained by triplicate determinations, and each data set was repeated at least two times.

not shown) that the biphasic profile was still obtained and that its maximum remains at 40% PE, which reinforces the argument that the position of the maximum is a function of the enzyme and not the bilayer. To investigate if the peptide substrates had any role in the biphasic activity profiles, the substrates were exchanged. The PKC $\epsilon$  pseudosubstrate peptide still produced a biphasic profile for PKC $\alpha$ , while MBP<sub>4–14</sub> still failed to do so for PKC $\epsilon$ , and both the MBP<sub>4–14</sub> and PKC $\epsilon$  pseudosubstrate produced biphasic profiles for PKC $\delta$  (results not shown).

**The Biphasic Activity Dependency as a Function of PE Content Is Not Due to Varied PKC Membrane Association.** To investigate whether the amount of PKC bound to the membrane lipid vesicles varied with PE content, and might therefore explain the biphasic effect on activity, membrane association of PKC was examined. The amount of PKC binding to vesicles as a function of varying PE content is shown in Figure 2. PKC $\alpha$ , PKC $\delta$ , and the PKC $\alpha$ -C1 domain were found to be essentially maximally membrane-bound at 0% PE, and the amount bound did not vary significantly as a function of POPE. For PKC $\epsilon$  and PKC $\zeta$  no biphasic profile was apparent (result not shown); in addition, membrane binding appears to be weaker and full association was not obtained. For PKC $\delta$ , PKC $\epsilon$ , PKC $\zeta$ , and PKC $\delta$ -C1, the presence of  $\text{Ca}^{2+}$  had no effect on binding or activity. A control which was treated identically, except without vesicle addition, showed no loss of PKC activity. We were also able to verify a lack of involvement binding in the biphasic features of PKC-vesicle interactions using Biacore 2000



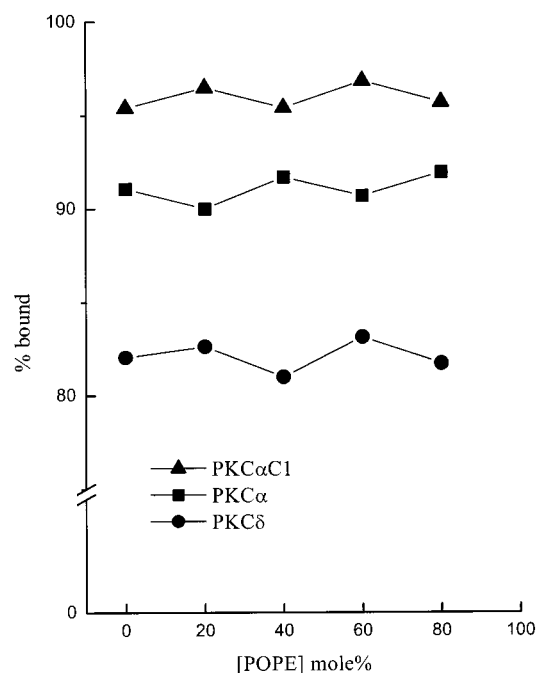


FIGURE 2: POPE concentration dependence of the degree of membrane lipid vesicle association of PKC $\alpha$ , PKC $\delta$ , and PKC $\alpha$ -C1. Vesicle compositions were as described in the legend of Figure 1 but were sucrose loaded to aid centrifugal separation of vesicle-bound from unbound PKC-C1 as described under Materials and Methods. The percentage of membrane-associated PKC was calculated on the basis of the PKC activity in the supernatant before and after centrifugation and is shown for PKC $\alpha$  (■) and PKC $\delta$  (●) or for the PKC $\alpha$ -C1 (▲), which was based on protein determination. The results show that POPE did not influence the amount of PKC-C1 bound.

surface plasmon resonance methodology. Binding data were obtained by tethering vesicles to a hydrophobic L1-pioneer chip surface, across which PKC was flowed. From preliminary experiments it is clear that much information can be obtained by this method (S. J. Slater and C. D. Stubbs, unpublished observations). At the moment we can only report here the preliminary observation of a lack of biphasic properties in any of the parameters obtained, confirming the centrifugation binding data. Further experimentation using this approach is in progress.

**PKC-Lipid Interaction Probed by the Fluorescence Anisotropy of Dansyl-PS Reveals a Biphasic Profile as a Function of PE Content for PKC $\alpha$ .** Dansyl-PS was introduced into the membrane lipids to probe the lipid dynamics at the PKC-lipid interfacial region adjacent to PKC in the membrane as modified by the different physical environments resulting from varied PE content. This was measured in terms of the fluorescence anisotropy. The data in Figure 3 represent the fluorescence anisotropy of dansyl-PS in lipids alone subtracted from the value after addition of PKC, with Ca<sup>2+</sup> for cPKC, without Ca<sup>2+</sup> for PKC $\epsilon$ , PKC $\delta$ , and PKC $\zeta$ , and without TPA for PKC $\zeta$ . By this means the contribution of the increase found in dansyl-PS anisotropy for the lipids alone as a function of PE (in the absence of PKC) was removed. The cPKC but not nPKC $\delta$  and PKC $\epsilon$ , or aPKC $\zeta$  isoforms, produced a biphasic profile of the increased anisotropy induced by PKC that was already maximally bound to the membrane.

**The Isolated C1 Domain of PKC $\alpha$  Displays a Biphasic Dansyl-PS Fluorescence Anisotropy Profile as a Function**

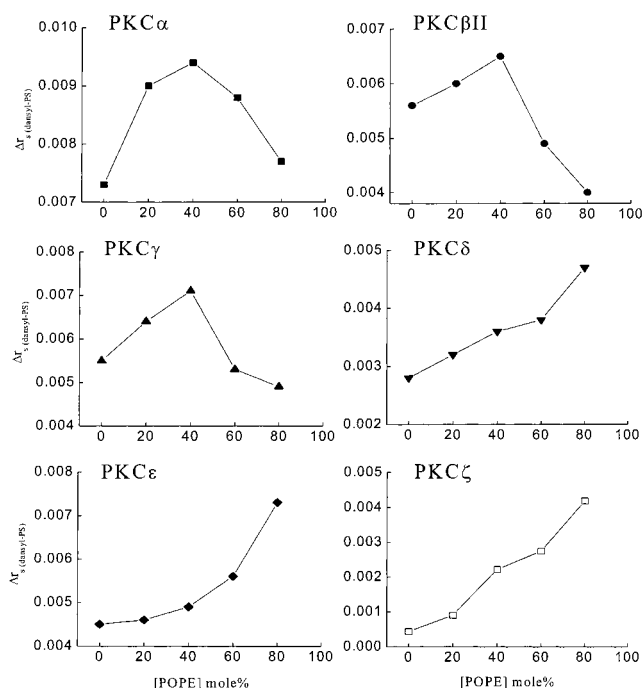


FIGURE 3: Effect of PE on the increase in the fluorescence anisotropy of dansyl-PS ( $\Delta r_s$ ) induced by the presence of the PKC. Vesicle compositions were as described in the legend of Figure 1.  $\Delta r_s$  is the differential anisotropy change upon addition of PKC. For cPKC, the value corresponds to the difference between  $r_s$  measured after and before the addition of 100  $\mu$ M Ca<sup>2+</sup>. For Ca<sup>2+</sup>-independent PKC, the value corresponds to the difference between  $r_s$  measured after and before the addition of PKC. PKC $\alpha$  (■), PKC $\beta$ II (●), and PKC $\gamma$  (▲) displayed biphasic POPE concentration dependencies whereas PKC $\delta$  (▼), PKC $\epsilon$  (◆), and PKC $\zeta$  (□) show increased  $\Delta r_s$  with increasing POPE content. For details see Materials and Methods.

**of PE Content.** The fluorescence anisotropy was then determined as a function of PE content for a fixed concentration of the PKC $\alpha$ -C1 domain, and a biphasic profile was again obtained as for intact PKC $\alpha$ , as shown in Figure 4. The inset in Figure 4 shows an example of the raw data from which each point was obtained. By contrast, there was a decrease in the fluorescence anisotropy with increasing PE for the C1 domains of PKC $\delta$  and PKC $\epsilon$ , Ca<sup>2+</sup> addition having no effect.

**The Rotational Correlation Time of the PKC-Bound Fluorescent Phorbol Ester SAPD Is a Biphasic Function of PE Content for Full-Length PKC $\alpha$  and PKC $\delta$ .** In a recent paper we reported that the rotational correlation time of the PKC-bound fluorescent phorbol ester SAPD increased with higher PE and cholesterol content in the lipid vesicles (5). The levels of PE high enough to reveal a biphasic relationship were not explored. The longer correlation time implies a motionally restricted phorbol ester binding pocket as expected. To obtain a correlation time for the PKC-bound fluorophore, the phase/modulation time-resolved anisotropy data for SAPD were analyzed, as previously, assuming a contribution of three components: a short correlation time (<1 ns) that can be ascribed to free SAPD, an 8–12 ns correlation time for SAPD in the lipid bilayer, and a longer 40–80 ns correlation time that arises from SAPD tightly bound to the C1 domain of PKC (5). The long rotational correlation time, corresponding to PKC $\alpha$ -bound SAPD, was a biphasic profile of PE content when examined over the 0–80% range (Figure 5a), as was the rotational correlation

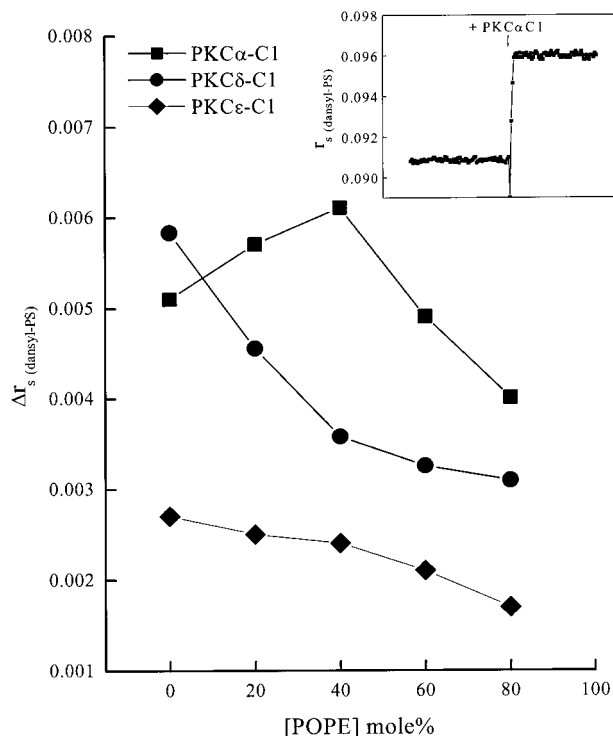


FIGURE 4: Effect of PE on the increase in the fluorescence anisotropy of dansyl-PS ( $\Delta r_s$ ) induced by the presence of the PKC-C1 domain. Vesicle compositions were as described in the legend of Figure 1.  $\Delta r_s$  is the differential anisotropy corresponding to the anisotropy without the C1 domain subtracted from that with the C1 domain.  $\text{Ca}^{2+}$  had no effect and was therefore omitted. For PKC $\alpha$ -C1 (■) a biphasic function with respect to POPE content was obtained (the C1 concentration was 20 nM). PKC $\delta$ -C1 (●) and PKC $\epsilon$ -C1 (◆) showed a decreased  $\Delta r_s$  with increasing POPE. For details see Materials and Methods.

time of PKC $\delta$ -bound SAPD (Figure 5b). Measurements of SAPD correlation time complexed with PKC $\epsilon$  were not made due to its low affinity for PKC $\epsilon$ , as reported elsewhere (47) and confirmed in separate experiments (F. J. Taddeo, S. J. Slater, and C. D. Stubbs, unpublished observations). PKC $\zeta$  also does not bind phorbol esters and could not be examined in this way. Previously, we showed that the rotational correlation time of SAPD complexed to the PKC $\alpha$ -C1 domain differed little from that measured for SAPD in a lipid bilayer (5); therefore, it was not possible to extract the SAPD rotational correlation time as a function of PE content for C1 domains.

*Effect of PKC Activity as a Function of Cholesterol Content Is Biphasic in the Presence of a Fixed Level of PE.* Apart from PE, the other major membrane lipid bilayer destabilizing component that influences PKC activity is cholesterol (14, 15, 48). In addition, cholesterol is known to promote nonbilayer structures in the presence of PE (49). Therefore, we reasoned that the effects of PE and cholesterol might be *additive* in terms of PKC activity. PKC $\alpha$  activity in the presence of 20 mol % PE as a function of cholesterol content is shown in Figure 6a. This also served as a control to demonstrate that the effects were not due to specific interactions with PE. Without PE, PKC $\alpha$  activity is increased as a function of cholesterol content, whereas with PE activity peaked at 20 mol % cholesterol, again yielding a biphasic profile. In keeping with this observation, the effect on the fluorescence anisotropy of dansyl-PS which also increased

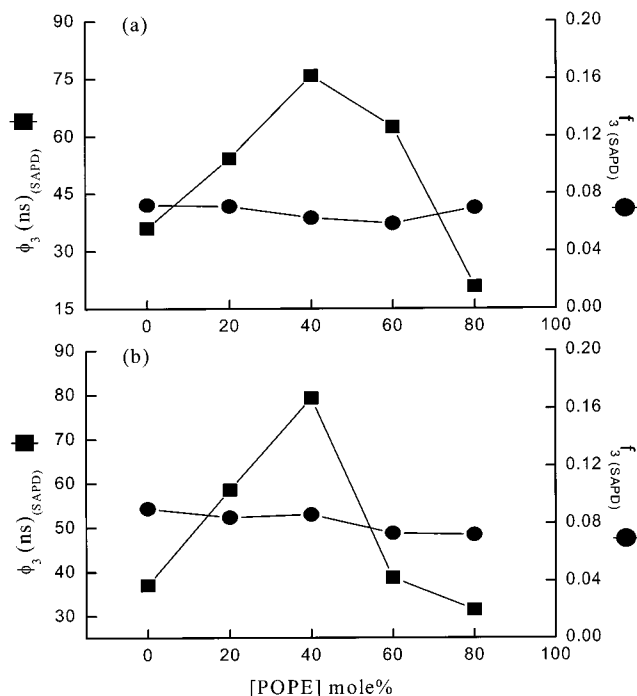


FIGURE 5: Rotational freedom of the fluorescent phorbol ester SAPD bound to the C1 domain as a function of PE content. The vesicle compositions were as described in the legend of Figure 1. (a) Rotational correlation time of PKC $\alpha$ -bound SAPD and its fractional contribution to the total SAPD as a function of POPE content. (b) Rotational correlation time and fractional contribution of PKC $\delta$ -bound SAPD as a function of POPE content. Both PKC $\alpha$ - and PKC $\delta$ -bound SAPD displayed a biphasic dependence of the rotational correlation time as a function of PE content. Time-resolved fluorescence anisotropy data were measured and analyzed as described under Materials and Methods.

with cholesterol again peaked at ~20 mol % cholesterol in the presence of 20 mol % PE (Figure 6b).

## DISCUSSION

In this study the origin of the sensitivity of PKC to the content of nonbilayer lipids in membranes was investigated. Previously, we showed that for a mixed cPKC isoform preparation activity increased with PE content to a maximum after which it declined (14). Here, it was found that the cPKC isoforms ( $\alpha$ ,  $\beta$ II, and  $\gamma$ ) along with PKC $\delta$ , but not PKC $\epsilon$  and aPKC $\zeta$ , displayed the same biphasic activity profile as a function of PE content, suggesting that while a functional C1 domain is required, a C2 domain is not required since only cPKC possesses the C2 domain. The latter was supported by the finding that, like the intact enzyme, the isolated C1 domain alone also exhibited a biphasic profile in terms of the dynamics of an adjacent lipid probe as well as by the dynamics of the fluorescent phorbol ester SAPD.

The results shown here build on previous studies showing that membrane-associated protein functions are sensitive to bilayer-destabilizing lipid content. Previous studies showed that increases in the hexagonal phase forming propensity of the membrane lipid bilayer, as induced by increased PE, lead to an increase the activity of PKC (5, 14, 50). The phospholipids having the lowest bilayer-hexagonal phase transition temperature being most effective in augmenting the activity of PKC (51). PE is a "conical shaped" lipid, compared to the cylindrical shape for PC, so that its small

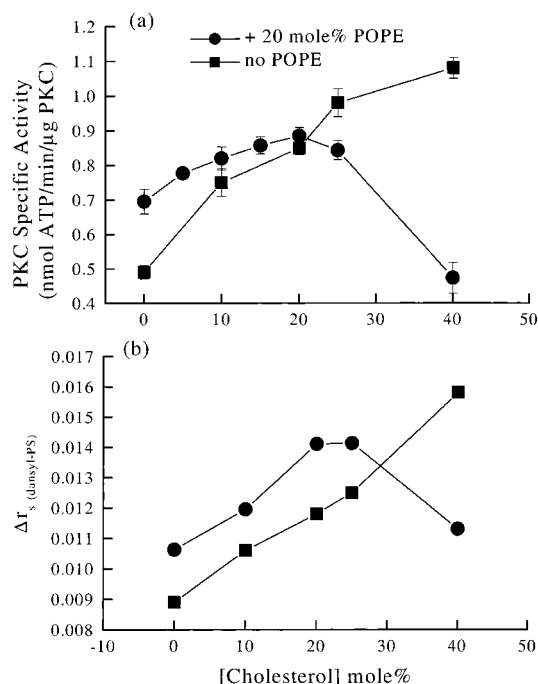


FIGURE 6: PKC activity and dansyl-PS fluorescence anisotropy as a function of cholesterol content dependency on the presence of PE. (a) PKC $\alpha$  activity and (b) the Ca<sup>2+</sup>-dependent dansyl-PS fluorescence anisotropy increase were biphasic as a function of cholesterol concentration only in the presence of PE. The vesicle compositions were as described in the legend of Figure 1, increased proportions of cholesterol being at the expense of decreased POPC, and  $\Delta r_s$  was determined as described in the legend of Figure 3. For details see Materials and Methods.

headgroup region yields a looser lipid packing and a resultant promotion of PKC insertion (14, 52). We proposed that as PKC inserts deeper into the bilayer, promoted by increased PE content, its conformation changes, there being a certain conformation that produces maximal activity at a specific PE level (14). Still further increases in PE may lead to a greater PKC insertion but may result in a conformation that is suboptimal, in terms of enzyme activity, explaining the biphasic activity profiles obtained. It is important to note that these effects are independent of PKC-membrane association which is maximal under varying PE content as shown here. The region of the PKC molecule involved and the PKC isoform specificity of the effect have remained to be explored.

No single global membrane physical parameter, such as lipid order (14), or the intrinsic radius of curvature ( $R_0$ ), elastic bending modulus, or the curvature strain energy of each monolayer (53), has emerged that might correlate with the effects of bilayer destabilization on PKC activity. In the present study we therefore took a different approach and examined *local* physical parameters using dansyl-PS fluorescence anisotropy to probe PKC region *adjacent* to the membrane lipids and the fluorescent phorbol ester SAPD to probe the *internal* dynamics of PKC in the C1 domain. While dansyl-labeled lipids have been used to assess the extent of PKC-membrane association, this is the first work to our knowledge that describes fluorescent phospholipids as probes of the hydrophobic surface of PKC, at the lipid-interface, as it responds to different lipid structures that influence activity. PKC $\alpha$  is fully membrane-bound at low Ca<sup>2+</sup> ( $\sim 1 \mu\text{M}$ ), yet appreciable activity requires higher levels in the 10–100  $\mu\text{M}$

region (7). Using PKC-tryptophan to dansyl-PE resonance energy transfer, we noted an increase in the RET signal as a function of Ca<sup>2+</sup> concentration beyond the level at which full membrane association occurred (7), the increase correlating with the appearance of activity. This suggested that the *activating conformational change* (5, 7) from *inactive* membrane-bound PKC to *active* PKC is directly sensed by the dansylated lipids. Accordingly, under conditions of fully bound PKC (confirmed in separate experiments), and with Ca<sup>2+</sup> sufficient for maximal activity, we used the dansyl fluorescence anisotropy to probe the hydrophobic PKC-lipid interface as a function of PE content. As with activity, it was found that there was a biphasic dependence of dansyl-PS fluorescence anisotropy as a function of PE content.

Examination of the activity of PKC as a function of PE content revealed a maximum that is similar for the different PKC isoforms ( $\alpha$ ,  $\beta\text{II}$ ,  $\gamma$ , and  $\delta$ ) at  $\sim 40$ –60% PE. This suggests that the structural feature in PKC responsible for PE sensitivity is conserved across cPKC and nPKC $\delta$  isoforms. The fact that the phenomenon is seen in nPKC $\delta$ , which lacks a conventional C2-Ca<sup>2+</sup>-binding domain, would suggest that the C1 rather than the C2 domain may be the lipid sensing module. Examination of the fluorescence anisotropy of dansyl-PS, for varying PE with the isolated PKC $\alpha$ -C1 domain, again revealed a biphasic activity profile, supporting this contention. However, it is clear that the feature is not conserved in the C1 domain across all isoforms since a biphasic activity profile was not obtained with PKC $\epsilon$  and  $\zeta$ , correlating with the lack of biphasic characteristics in the dansyl-PS anisotropy.

A biphasic dansyl-PS fluorescence anisotropy profile was not obtained for intact PKC $\delta$  nor its isolated C1 domain, despite the biphasic activity profile. This suggests that the region of the PKC that experienced the conformational change detected by the dansyl probe in cPKC may not be optimally positioned at the protein-lipid interface in PKC $\delta$  where the dansyl resides. We therefore turned to the fluorescent phorbol ester SAPD to probe the conformation of the phorbol ester binding site within the C1 domain as a function of PE. It was found that the rotational correlation time of the PKC-bound SAPD was a biphasic profile as a function of PE for both full-length cPKC $\alpha$  and nPKC $\delta$ . It was not possible to extract a rotational correlation time for SAPD for the isolated C1 domains. This is probably due to the folding of the isolated C1 domain differing somewhat from when it resides as part of the full-length protein. Thus the C1-bound SAPD for full-length PKC of about  $\sim 40$  ns drops to around  $\sim 8$  ns for the isolated C1 domain which cannot be resolved from the value for SAPD in lipids of  $\sim 9$  ns (5). Despite this, the finding that both the fluorescence anisotropy of dansyl-PS and the rotational correlation time of the full-length PKC $\alpha$  (C1 domain) bound-SAPD were a biphasic function of PE content strongly implicate the C1 domain as the “lipid sensing module” at least for cPKC isoforms and possibly also for PKC $\delta$ . The possibility that SAPD binds to other parts of the PKC molecule has been previously discounted (7, 8, 40). Finally, it is important to note that, without PKC, neither the dansyl-PS anisotropy nor SAPD rotational correlation time followed a biphasic relationship in the lipids alone as a function of PE content.

Other studies on the C1 domain support its importance in directing the activation of PKC. In structural studies of the



PKC $\delta$  C1 domain it was suggested that the interaction with a phorbol ester caps a hydrophobic pocket facilitating interaction with the membrane (54). More recently, it was pointed out (55) that the C1a domain is adjacent to the pseudosubstrate region so that the conformational changes that accompany penetration of the C1a domain into the membrane probably provide the mechanical force to allow the removal of the pseudosubstrate to reveal the substrate binding site. It was shown that the membrane-penetrating power of the C1 domain in the PKC is by default restrained by other parts of the molecule until activated. It was also pointed out that the high affinity of the isolated C1 domain for phorbol dibutyrate shows that it is functionally folded, ruling out the possibility that its high monolayer penetration power was due to the incomplete folding of the C1 domain in isolation. Further, it was suggested that it is the C1a domain that is *required* for membrane penetration and activation (of PKC $\alpha$ ) and that it contains the DAG-binding pocket that is *distinct* from the phorbol ester binding pocket which may be the C1b domain (55), an observation in keeping with our low and high phorbol ester affinity binding site model (8). Which of the C1a or C1b region or both might constitute the nonbilayer lipid destabilization sensing module remains to be determined; however, the effects of mutations on the monolayer penetration of PKC show that the upper part of the C1a but not the C1b domain penetrates into the membrane (55), perhaps implicating the former.

PKC activity also displays a biphasic profile as a function of PS concentration with PC/PS vesicles (56). The results were again consistent with the C1 but not the C2 domain being responsible for this phenomenon, as in the present study, since it was again found with both the PKC $\alpha$  and PKC $\delta$ , the latter not containing a C2 domain. Whether C1 domains have a role in the process remains to be determined. Elsewhere a biphasic profile for activity has also been reported for systems containing high levels of DAG and fatty acids (57). It was suggested that while increasing activity correlated with increasing bilayer "frustration", i.e., increasing content of lipid that favors nonbilayer phases, then for increasing presence of nonbilayer lipid formation activity declines, although the latter would be unlikely to occur in POPE systems as used here. The fact that biphasic profiles are formed as a function of lipid (PS) concentration has led to the suggestion that PKC-PKC interactions may be involved in the effect (56), and elsewhere evidence for such has appeared (58).

The results of this study have important implications both for the understanding of how PKC is regulated and for designing novel approaches to modulate its activity. The question that is left to answer is what are the reasons for the isoform differences in the biphasic response. At present we can only speculate that the nonconserved amino acids in the different PKC isoforms are conferring a different conformational response in the PKC's leading to enzyme activities the precise nature of which await further study. Clearly understanding the C1-activator binding domain is a key to the regulation of PKC activity since both the chemical structure of the activator molecule (DAG, phorbol ester or other) and the structural interaction between the PKC and the membrane surface are directed by this module.

## ACKNOWLEDGMENT

We thank Dr. Peter Blumberg for providing the plasmid of PKC $\delta$ -C1. We are indebted to Anthony Cook, Jennifer Reppert, and Jodie Seiz for technical support.

## REFERENCES

1. Jaken, S. (1996) *Curr. Opin. Cell Biol.* 8, 168–173.
2. Mellor, H., and Parker, P. J. (1998) *Biochem. J.* 332, 281–292.
3. Nishizuka, Y. (1995) *FASEB J.* 9, 484–496.
4. Newton, A. C., and Johnson, J. E. (1998) *Biochim. Biophys. Acta* 1376, 155–172.
5. Ho, C., Slater, S. J., Stagliano, B. A., and Stubbs, C. D. (1999) *Biochem. J.* 344 (Part 2), 451–460.
6. Stubbs, C. D., and Slater, S. J. (1996) *Chem. Phys. Lipids* 81, 185–195.
7. Slater, S. J., Milano, S. K., Stagliano, B. A., Gergich, K. J., Ho, C., Mazurek, A., Taddeo, F. J., Kelly, M. B., Yeager, M. D., and Stubbs, C. D. (1999) *Biochemistry* 38, 3804–3815.
8. Slater, S. J., Ho, C., Kelly, M. B., Larkin, J. D., Taddeo, F. J., Yeager, M. D., and Stubbs, C. D. (1996) *J. Biol. Chem.* 271, 4627–4631.
9. Slater, S. J., Kelly, M. B., Taddeo, F. J., Rubin, E., and Stubbs, C. D. (1994) *J. Biol. Chem.* 269, 17160–17165.
10. Kaibuchi, K., Takai, Y., and Nishizuka, Y. (1981) *J. Biol. Chem.* 256, 7146–7149.
11. Epand, R. M., and Bottega, R. (1988) *Biochim. Biophys. Acta* 944, 144–154.
12. Orr, J. W., and Newton, A. C. (1992) *Biochemistry* 31, 4661–4667.
13. Bazzi, M. D., Youakim, M. A., and Nelsestuen, G. L. (1992) *Biochemistry* 31, 1125–1134.
14. Slater, S. J., Kelly, M. B., Taddeo, F. J., Ho, C., Rubin, E., and Stubbs, C. D. (1994) *J. Biol. Chem.* 269, 4866–4871.
15. Bolen, E. J., and Sando, J. J. (1992) *Biochemistry* 31, 5945–5951.
16. Kano-Sueoka, T., and Nicks, M. E. (1993) *Cell Growth Differ.* 4, 533–537.
17. Gavrilova, N. J., Markovska, T. T., Momchilova-Pankova, A. B., Setchenska, M. S., and Koumanov, K. S. (1992) *Biochim. Biophys. Acta* 1105, 328–332.
18. Nikolova-Karakashian, M. N., Gavrilova, N. J., Petkova, D. H., and Setchenska, M. S. (1992) *Biochem. Cell. Biol.* 70, 613–616.
19. Sen, A., Isac, T. V., and Hui, S. W. (1991) *Biochemistry* 30, 4516–4521.
20. Buckley, J. T. (1985) *Can J. Biochem. Cell Biol.* 63, 263–267.
21. Rao, N. M., and Sundaram, C. S. (1993) *Biochemistry* 32, 8547–8552.
22. Burack, W. R., and Biltonen, R. L. (1994) *Chem. Phys. Lipids* 73, 209–222.
23. Kinnunen, P. K. J. (1996) *Chem. Phys. Lipids* 81, 151–166.
24. Cullis, P. R., and de Kruijff, B. (1979) *Biochim. Biophys. Acta* 559, 399–420.
25. Rietveld, A. G., Chupin, V. V., Koorengevel, M. C., Wienk, H. L., Dowhan, W., and de Kruijff, B. (1994) *J. Biol. Chem.* 269, 28670–28675.
26. Matsuzaki, K., Sugishita, K., Ishibe, N., Ueha, M., Nakata, S., Miyajima, K., and Epand, R. M. (1998) *Biochemistry* 37, 11856–11863.
27. Scarlata, S., and Gruner, S. M. (1997) *Biophys. Chem.* 67, 269–279.
28. Huang, H., Ball, J. M., Billheimer, J. T., and Schroeder, F. (1999) *Biochem. J.* 344, 593–603.
29. Heimburg, T., Hildebrandt, P., and Marsh, D. (1991) *Biochemistry* 30, 9084–9089.
30. Razinkov, V. I., Melikyan, G. B., Epand, R. M., Epand, R. F., and Cohen, F. S. (1998) *J. Gen. Physiol.* 112, 409–422.
31. Lewis, J. R., and Cafiso, D. S. (1999) *Biochemistry* 38, 5932–5938.

32. Cornell, R. B., and Arnold, R. S. (1996) *Chem. Phys. Lipids* 81, 215–228.
33. Yang, F. Y., and Hwang, F. (1996) *Chem. Phys. Lipids* 81, 197–202.
34. Gruner, S. M. (1985) *Proc. Natl. Acad. Sci. U.S.A.* 82, 3665–3669.
35. Tate, M. W., Eikenberry, E. F., Turner, D. C., Shyamsunder, E., and Gruner, S. M. (1991) *Chem. Phys. Lipids* 57, 147–164.
36. Bartlett, G. R. (1959) *J. Biol. Chem.* 234, 466–468.
37. MacDonald, R. C., MacDonald, R. L., Menco, B. P., Takeshita, K., Subbarao, N. K., and Hu, L. R. (1991) *Biochim. Biophys. Acta* 1061, 297–303.
38. Stabel, S., Schaap, D., and Parker, P. J. (1991) *Methods Enzymol.* 200, 670–673.
39. Taddeo, F. J. (1998) Cloning, expression and purification of protein kinase C: A comparative study of the modes of activation of protein kinase C, Ph.D. Thesis, Thomas Jefferson University.
40. Slater, S. J., Taddeo, F. J., Mazurek, A., Stagliano, B. A., Milano, S. K., Kelly, M. B., Ho, C., and Stubbs, C. D. (1998) *J. Biol. Chem.* 273, 23160–23168.
41. Bogi, K., Lorenzo, P. S., Szallasi, Z., Acs, P., Wagner, G. S., and Blumberg, P. M. (1998) *Cancer Res.* 58, 1423–1428.
42. Mosior, M., and Epand, R. M. (1994) *J. Biol. Chem.* 269, 13798–13805.
43. Gratton, E., Jameson, D. M., and Hall, R. D. (1984) *Annu. Rev. Biophys. Bioeng.* 13, 105–124.
44. Lakowicz, J. R., Gratton, E., Cherek, H., Maliwal, B. P., and Laczko, G. (1984) *J. Biol. Chem.* 259, 10967–10972.
45. Beechem, J. M. (1989) *Chem. Phys. Lipids* 50, 237–251.
46. Beechem, J. M. (1992) *Methods Enzymol.* 210, 37–54.
47. Dimitrijevic, S. M., Ryves, W. J., Parker, P. J., and Evans, F. J. (1995) *Mol. Pharmacol.* 48, 259–267.
48. Haefner, E. W., and Wittmann, U. (1994) *Cell Signal.* 6, 201–207.
49. Tilcock, C. P., Bally, M. B., Farren, S. B., and Cullis, P. R. (1982) *Biochemistry* 21, 4596–4601.
50. Epand, R. M., Epand, R. F., Leon, B. T., Menger, F. M., and Kuo, J. F. (1991) *Biosci. Rep.* 11, 59–64.
51. Senisterra, G., and Epand, R. M. (1993) *Arch. Biochem. Biophys.* 300, 378–383.
52. Epand, R. M., Stafford, A. R., and Lester, D. S. (1992) *Eur. J. Biochem.* 208, 327–332.
53. Giorgione, J. R., Kraayenhof, R., and Epand, R. M. (1998) *Biochemistry* 37, 10956–10960.
54. Zhang, G., Kazanietz, M. G., Blumberg, P. M., and Hurley, J. H. (1995) *Cell* 81, 917–924.
55. Medkova, M., and Cho, W. (1999) *J. Biol. Chem.* 274, 19852–19861.
56. Sando, J. J., Chertihin, O. I., Owens, J. M., and Kretsinger, R. H. (1998) *J. Biol. Chem.* 273, 34022–34027.
57. Goldberg, E. M., and Zidovetzki, R. (1998) *Biochemistry* 37, 5623–5632.
58. Huang, S. M., Leventhal, P. S., Wiepz, G. J., and Bertics, P. J. (1999) *Biochemistry* 38, 12020–12027.

BI002839X